
This is an electronic reprint of the original article.
This reprint may differ from the original in pagination and typographic detail.

Andersson, Stefan; Holopainen, Jari; Kuosmanen, Matti
Beam Steering Performance Improvements Using a Layered Permittivity Dielectric

Published in:
18th European Conference on Antennas and Propagation, EuCAP 2024

DOI:
[10.23919/EuCAP60739.2024.10500957](https://doi.org/10.23919/EuCAP60739.2024.10500957)

Published: 01/01/2024

Document Version
Publisher's PDF, also known as Version of record

Please cite the original version:
Andersson, S., Holopainen, J., & Kuosmanen, M. (2024). Beam Steering Performance Improvements Using a Layered Permittivity Dielectric. In *18th European Conference on Antennas and Propagation, EuCAP 2024* IEEE. <https://doi.org/10.23919/EuCAP60739.2024.10500957>

This material is protected by copyright and other intellectual property rights, and duplication or sale of all or part of any of the repository collections is not permitted, except that material may be duplicated by you for your research use or educational purposes in electronic or print form. You must obtain permission for any other use. Electronic or print copies may not be offered, whether for sale or otherwise to anyone who is not an authorised user.

Beam Steering Performance Improvements Using a Layered Permittivity Dielectric

Stefan Andersson, Jari Holopainen, Matti Kuosmanen,
Department of Electronics and Nanotechnology, Aalto University, Espoo, Finland,
stefan.andersson@aalto.fi

Abstract—This paper presents simulated performance improvements utilizing a layered dielectric for a truncated tapered slotline array targeted in the 2 – 7 GHz frequency range. It will be shown that a dielectric loading may significantly improve the bandwidth and beam-steering characteristics of the antenna array. Furthermore, it will be demonstrated that a layered dielectric structure with different permittivities can further improve the performance compared to a homogeneous dielectric. Namely, the antenna with layered dielectrics display a further increase in bandwidth and wider beam steering angles in the H-plane.

Index Terms—antenna simulation, beam steering, dielectric, simulation, vivaldi.

I. INTRODUCTION

The ever increased prevalence of 3D-printing makes it very appealing to find novel ways to take advantage of additive manufacturing methods. Subsequently, the challenge becomes finding performance improvements in antenna applications by taking advantage of innovative dielectric structures. Dielectrics loading may for instance be used to reduce antenna size [1]. One example of this is a layered dielectric structure made from one host material [2]. A monolithic layered permittivity structure can be manufactured by controlling the fraction of material to air. In other words, by printing a dielectric with specifically designed cavities, or inclusions, that reduce the effective permittivity of the material to a desired value lower than the host material. This of course has the inherent issue of being rather challenging to simulate, because it generates a huge mesh size for otherwise relatively simple structures. However, there are certainly numerous other methods to achieve a similar effect, such as a grid structure [3]. That said, an artificial material like this can be approximated as an isotropic material if the inclusions are sub-wavelength [4]. In this research, that assumption is made, and the material layers are approximated as solid dielectric blocks. Thus, the exact method to achieve this will not be discussed further.

In this paper, we compare the simulated results of three different tapered slotline antenna models. The first antenna model serves as a free space reference model without any dielectric loading. The second antenna model is encased in a homogeneous dielectric material, also serving as a reference. A third approach is then proposed where the dielectric is comprised of three layers of material with different dielectric constants, chosen to reproduce effective permittivity materials with the same host material as in the second antenna model.

In both cases, we only consider a planar dielectric structure in front of the tapered slotline element.

II. SIMULATIONS

The coplanar tapered slot element was chosen because it is a ubiquitous antenna type with wide bandwidth characteristics, and it is simple to model. The exponential tapering of the slot is defined by the function [5]

$$z(y) = \pm \frac{1}{2} w_{\min} e^{py}, \quad (1)$$

and the other end of the slot is terminated with a resonant area, which in this case is used for matching. For a viable comparison between the antenna models with and without being dielectric-loaded, the feed structure was omitted from the simulations, and a discrete port was instead used for excitation. The metallic structure was set on a 1.55 mm thick FR-4 substrate with a dielectric constant of $\epsilon_r = 4.3$, and a loss tangent of $\tan \delta = 0.025$. The metallic structure is simulated as copper. There is no common ground plane behind the elements.

The three antenna models were simulated with the help of unit cell simulations in CST Studio Suite [6], with a periodicity of $w_{\text{ele}} \times w_{\text{ele}}$ in the xy -plane. For the dielectric-loaded models, a number of permittivities were used, with a common loss tangent of $\tan \delta = 0.001$, representative of a general radome-grade 3D-printable dielectric, for instance [7].

The common design goal for the three antenna models was a bandwidth as wide as possible in the range of 2–7 GHz, with an active reflection coefficient (ARC) of less than -10 dB, and beam-steering angles of $\pm 50^\circ$. Each of the three cases were individually optimized to provide as wide as possible bandwidth, while analyzing the resulting beam-steering performance.

A. Free Space Reference

To provide a baseline of the performance without any dielectric loading, a tapered slot antenna array was simulated with free space between the elements in the x -dimension. The unit cell of the free space reference model in the yz -plane can be seen in Fig. 1. The position of the discrete port is marked with a red dot, and the corresponding dimensional values are summarized in Table I.

The ARC of the free space reference can be seen in Fig. 2 in the E-, H-, and D-planes. The ARC measures the reflection coefficient of a single element in the array when taking into

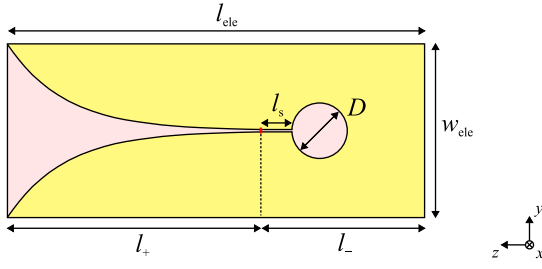


Fig. 1. The free space reference unit cell in the yz -plane.

TABLE I
FREE SPACE REFERENCE MODEL DIMENSIONS

Parameter	Description	Value (mm)
w_{ele}	Element width	22.5
w_{max}	Tapering maximum width	22.5
w_{min}	Slot gap	0.3
l_{ele}	Element length	54.0
l_+	Length above feed	31.8
l_-	Length behind feed	22.2
l_s	Slot length	5.0
D	Resonant area diameter	7.2

account the mutual coupling between the elements [8]. In the E-plane, the ARC is well-behaved with beam steering angles greater than $\pm 50^\circ$ within the 2 – 6 GHz range. In the D-plane, the scan angles are somewhat reduced, however, as the beam is scanned in the H-plane the performance significantly deteriorates.

B. Homogeneous Permittivity Loaded Reference

To study the effect of a homogeneous dielectric loading, the area between the PCBs in the x -dimension was filled with a material with a dielectric constant of $\epsilon_{r1} = 2.5$, creating a sandwich structure with the PCB in the middle of two dielectric blocks. The total thickness of the unit cell in the x -dimension is w_{ele} . Additionally, the area above the element in the z -direction was also filled with the same dielectric material, as shown in Fig. 3. The dimensions are displayed in Table II. Due to the addition of the dielectric, the length of

TABLE II
HOMOGENEOUS DIELECTRIC LOADED REFERENCE MODEL DIMENSIONS

Parameter	Description	Value (mm)
w_{ele}	Element width	22.7
w_{max}	Aperture width	21.5
w_{min}	Slot gap	0.3
l_{ele}	Element length	46.1
l_+	Length above feed	15.0
l_-	Length behind feed	21.1
l_s	Slot length	4.0
D	Resonant area diameter	5.0
d_1	Dielectric thickness above element	10.0

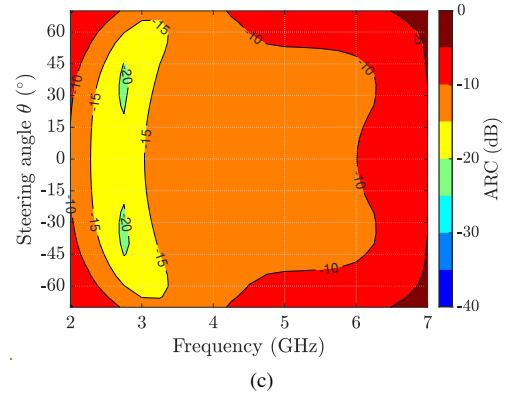
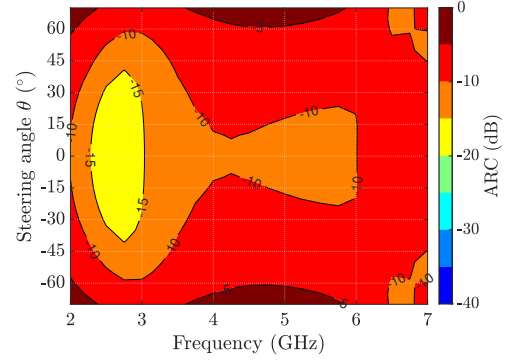
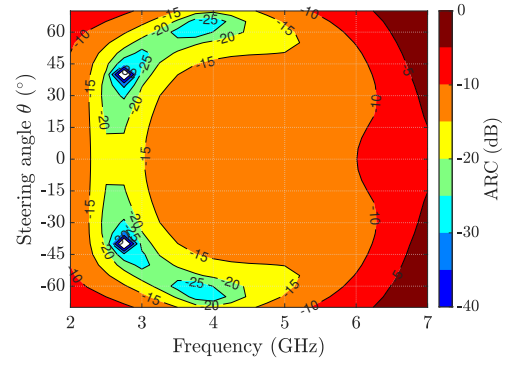


Fig. 2. The ARC of the free space reference in (a) the E-plane, (b) the H-plane, and (c) the D-plane.

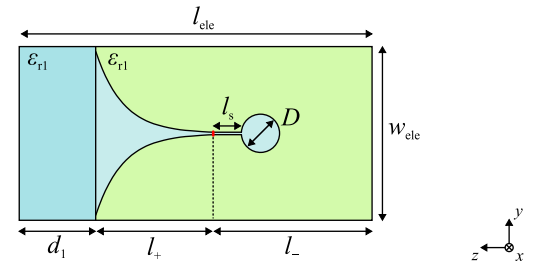


Fig. 3. The homogeneous permittivity unit cell in the yz -plane.

the tapered section l_+ was able to be reduced by 52.3% from 31.8 mm to 15 mm. Overall, the total length of the element

l_{ele} is shortened by 15% from 54.0 mm down to 46.1 mm. This has the important effect of significantly improving the beam-steering capability in the H-plane, as we can observe in Fig. 4b. We can also observe that the impedance bandwidth improved by 0.75 GHz in the broadside direction, and the scan angles in the D-plane improved significantly. In the H-plane, the ARC is below -10 dB for angles $\pm 50^\circ$ up to 4.75 GHz. However, the ARC quickly deteriorates for wider beam-steering angles as the frequency is increased.

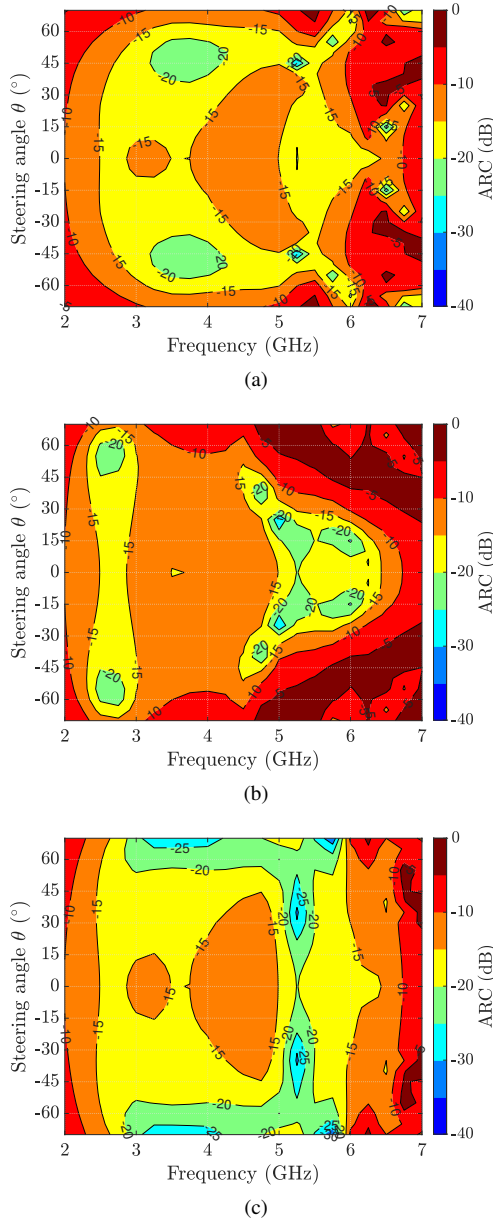


Fig. 4. The ARC of the homogeneous reference in (a) the E-plane, (b) the H-plane, and (c) the D-plane.

C. Layered Permittivity Model

For the layered permittivity model, the material between the PCBs remains the same $\epsilon_{r1} = 2.5$ as before, however the layer

above the element is now split into two layers of $\epsilon_{r2} = 2.0$ and $\epsilon_{r3} = 1.5$, the former being the middle layer and the latter the outermost layer. The structure can be seen in Fig. 5, and the respective parameters are detailed in Table III. In comparison to the homogeneous dielectric model, the metal structure stays approximately the same, with minor adjustments. To tune the structure, the element and aperture widths were slightly reduced, while the length of the tapered section was marginally increased. One of the significant advantages of the layered permittivity model is that it provides more design freedom, due to the additional impedance boundary layers that can be used to design a wider bandwidth antenna.

The ARC of the layered permittivity model is presented in Fig. 6. The most significant improvement compared to the homogeneous reference that can be observed is the improvement in beam-steering angles in the H-plane. Furthermore, we can observe an increase in impedance bandwidth in the broadside direction. Although the $\pm 50^\circ$ beam-steering angle design goal is not fulfilled over the entire frequency range in the H-plane, this factor could be improved by relaxing the bandwidth prerequisite. This could also help improve the ARC in the broadside around 5 GHz.

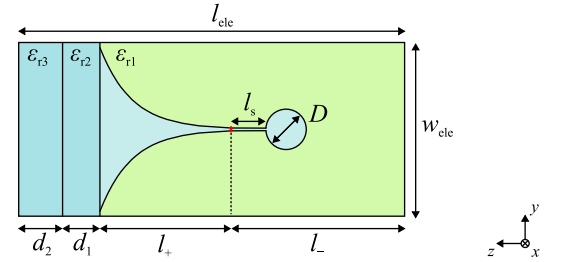


Fig. 5. The layered permittivity unit cell with three layers in the yz -plane.

TABLE III
LAYERED DIELECTRIC LOADED MODEL DIMENSIONS

Parameter	Description	Value (mm)
w_{ele}	Element width	21.4
w_{max}	Aperture width	20.2
w_{min}	Slot gap	0.3
l_{ele}	Element length	47.5
l_+	Length above feed	16.4
l_-	Length behind feed	21.1
l_s	Slot length	4.0
D	Resonant area diameter	5.0
d_1	First dielectric layer thickness	4.6
d_2	Second dielectric layer thickness	5.4

To get a better idea of the performance of the antenna arrays, we study the embedded element pattern (EEP). In the absence of grating lobes, the EEP is defined as

$$G(\theta, \phi) = \frac{4\pi A_{\text{phys}}}{\lambda_0^2} \cos \theta (1 - |\Gamma(\alpha, \beta)|^2), \quad (2)$$

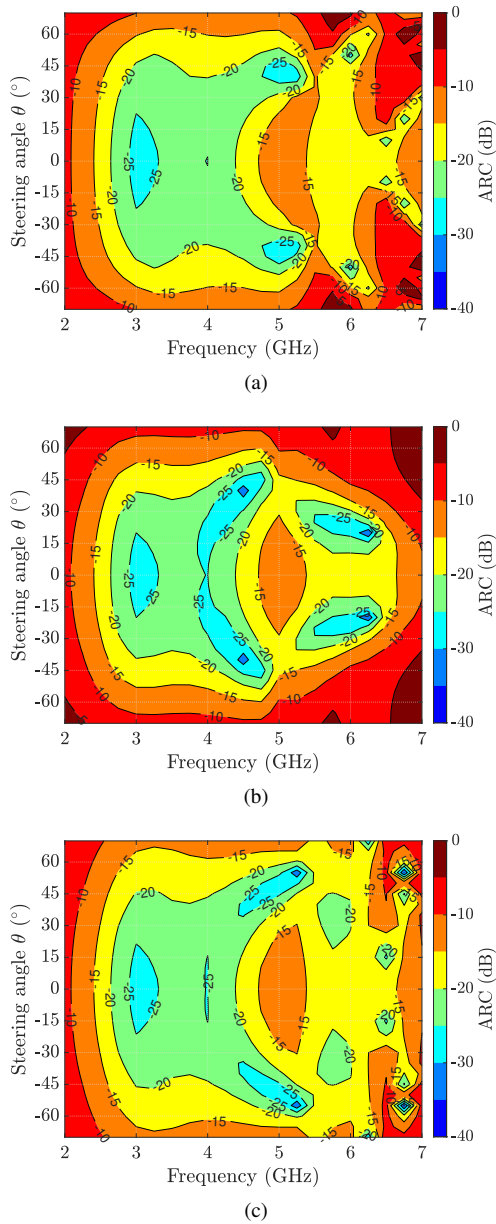


Fig. 6. The ARC of the layered permittivity model in (a) the E-plane, (b) the H-plane, and (c) the D-plane.

where θ is the scan angle, A_{phys} is the physical area of one element in the array, and $\Gamma(\alpha, \beta)$ is the ARC [9]. Equation (2) tells us that in a ideal reflectionless case at a given frequency and angle, the gain is limited by the element area. The embedded element patterns (EEP) of the three antenna elements are compared in Fig. 7. At 3 GHz, all three models are quite well behaved. The marginally worse performance of the layered model is due to the slightly narrower element, which decreases the potential realized gain according to (2). At 4.5 GHz, a dip in the homogeneous reference can be seen in the broadside direction, corresponding to the impedance mismatch in the ARC. Similar behaviour could be observed at around 5 GHz for the layered permittivity model. At 6 GHz, the most

significant improvement in beam-steering angles can be seen for the layered permittivity model when comparing to the poor performance of the homogeneous reference, especially in the H-plane. In Fig. 8, the realized gain in the broadside direction is compared to the theoretical gain obtained from (2) when the $\Gamma(\alpha, \beta) = 0$, that is, the simulated realized gain is compared to the potential maximum that is achievable. We can observe that in this regard the homogeneous dielectric model is more efficient than than free space model for frequencies below 4.25 GHz, and the layered dielectric model is more efficient than both below 4.75 GHz. However, both dielectric models suffer from a severe dip at around 5 GHz. This clearly correlates with the ARC in Figs. 4 and 6, and can be further explained by undesired radiation in the negative z -direction at these frequencies. The problem is less severe for the layered dielectric model, but nevertheless something that would have to be addressed in a practical antenna system.

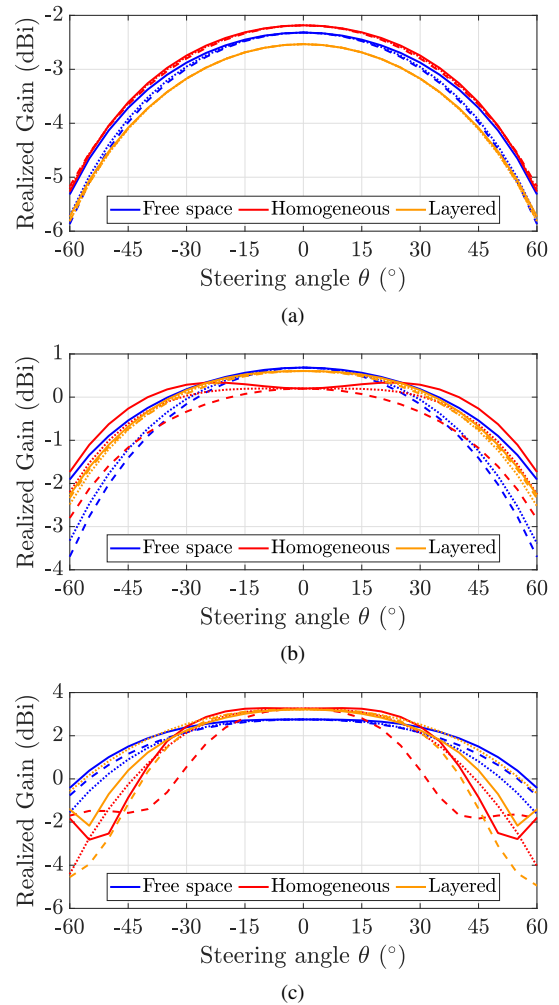


Fig. 7. A comparison of the EEP at (a) 3 GHz, (b) 4.5 GHz, and (c) 6 GHz. The solid lines shows the EEP in the E-plane, the dashed lines in the H-plane, and the dotted lines in the D-plane.

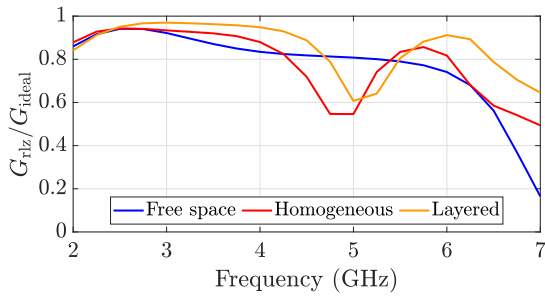


Fig. 8. Simulated realized gain compared to the ideal EEP in the broadside direction.

III. CONCLUSION

In this paper, the possible advantages of a variable dielectric structure has been shown. Through simulations it has been demonstrated that the bandwidth and beam-steering performance can be improved by applying a dielectric loading to a conventional tapered slotline antenna, and the performance can be further improved by using dielectric layers with different permittivity values. Furthermore, the reduced element height may be considered an additional benefit. The results also show that the dielectric loading helps to achieve a realized gain closer to the ideal value given by the physical area per element in the array.

ACKNOWLEDGMENT

This work has been carried out using Aalto Electronics-ICT infrastructure.

REFERENCES

- [1] L. Shafai, "Dielectric loaded antennas," in *Encyclopedia of RF and Microwave Engineering, Volumes 1 – 6*. Hoboken, NJ, USA: John Wiley & Sons, 2005, pp. 893–915.
- [2] H. F. Ma, B. G. Cai, T. X. Zhang, Y. Yang, W. X. Jiang and T. J. Cui, "Three-Dimensional Gradient-Index Materials and Their Applications in Microwave Lens Antennas," in *IEEE Trans. Antennas and Propag.*, vol. 61, no. 5, pp. 2561–2569, May 2013.
- [3] S. Zhang, P. Liu, and W. Whittow, "Design and fabrication of 3-D-printed high-gain broadband fresnel zone lens using hybrid groove-perforation method for millimeter-wave applications," *IEEE Antennas Wirel. Propag. Lett.*, vol. 21, no. 1, pp. 34–38, Jan. 2022.
- [4] A. H. Sihvola, *Electromagnetic Mixing Formulas and Applications*. London: Institution Of Electrical Engineers, 1999.
- [5] C. A. Balanis, *Antenna Theory Analysis and Design*, 4th ed. Hoboken, NJ, USA: Wiley, 2016.
- [6] *CST Studio Suite*, (2022), Dassault Systèmes Simulia Corp. Accessed: Oct. 13, 2022. [Online]. Available: <https://www.3ds.com/products-services/simulia/products/cst-studio-suite/>
- [7] "Radio Frequency Materials", Avient Corp. (2022), Accessed: Oct. 13, 2022. [Online]. Available: <https://www.avient.com/sites/default/files/2022-11/PREPERM%20RF%20Materials%201-pager.pdf>
- [8] R. C. Hansen, *Phased Array Antennas*, 2nd ed. Hoboken, NJ, USA: JohnWiley & Sons, 2009.
- [9] D. M. Pozar, "The active element pattern," *IEEE Trans. Antennas Propag.*, vol. 42, no. 8, pp. 1176–1178, Aug. 1994.